AUT Journal of Electrical Engineering

AUT J. Elec. Eng., 52(2) (2020) 179-186
DOI: 10.22060/eej.2020.18432.5353

Transmission and Reflection Characteristics of a Concrete Block Wall Illuminated by a TM-polarized Obliquely incident wave

A. Ahmadi[1], P. Dehkhoda[2,*], A. Tavakoli[3], and M. Dehmollaian[4]

[1]Ph.D. Candidate, Department of Electrical Engineering, Amirkabir University of Technology, Tehran, Iran
[2]Ph.D., Department of Electrical Engineering, Amirkabir University of Technology, Tehran, Iran
[3] Ph.D., Department of Electrical Engineering, Amirkabir University of Technology, Tehran, Iran
[4] Ph.D., School of Electrical and Computer Engineering, University of Tehran, Tehran, Iran

ABSTRACT: Typically, many of the modern buildings have concrete walls constructed from cinder block walls, that have periodic nature in their relative dielectric constant. This periodic nature excites higher-order Floquet harmonic modes at microwave frequencies, which leads to the propagation of scattered waves along with non-specular directions. Periodic structures exhibit different behaviors when illuminated by different types of incident polarizations. Previous studies mainly focus on the Transverse Electric (TE) incident wave, where the behavior of a periodic layer is characterized easily by only considering the function of the relative permittivity in the equations. But, for a Transverse Magnetic (TM) incident plane wave, the first-order derivative of the relative permittivity function must be taken into account in the formulations. Accordingly, in this paper, reflection and transmission coefficients from a typical concrete block wall are formulated for a TM polarized incident wave. Exact boundary equations are written, and the effect of oblique incidence is taken into account. Also, the periodic nature of the inhomogeneous layer is represented by the Fourier series. In addition, two types of numerical validation are provided to prove the accuracy of the given theory. The ability to calculate Fourier series coefficients by taking the Fast Fourier Transform (FFT) of the relative permittivity function enables the introduced method to treat any type of periodic inhomogeneities.

Review History:

Received: 2020-05-14
Revised: 2020-07-15
Accepted: 2020-07-19
Available Online: 2020-12-01

Keywords:

Concrete block-wall
Floquet modes
Periodic structure
Reflection and Transmission coefficients
TM-polarization

1. Introduction

Understanding the propagation mechanisms of the electromagnetic fields inside the walls of a building has been a topic of interest for decades. Growing use of wireless networks, from radio local area networks (LANs) to technology leading 4^{th} and 5^{th} generations of cellular networks, and the vital importance of behind- or through-the-wall imaging of humans and objects in crisis management, control, and security applications are some examples that show how important is to know the wave propagation through the walls as well as its scattering.

Periodic concrete cinder blocks are the constructing unit of common walls. Because of their periodicity, these walls can potentially scatter the reflected and transmitted waves along with non-specular directions, which must be considered carefully. In radar imaging applications [1]-[2], and wireless propagation modeling [3]-[8], characteristics of these periodic walls are studied mostly by the numerical and partly with the semi-analytical methods to find the scattering coefficients for both perpendicular (TE) and parallel (TM) incident polarizations. In the semi-analytical approaches, efforts have been made to study the reflection and transmission characteristics of concrete block walls for the TE polarized illumination [8]. In addition, properties of the modes in a medium that is periodic in one direction and is illuminated by a TE-polarized wave, have been formulated exactly in [9] and [10]. Other examples for TE-polarized incident wave are scattering from a rectangular room composed of concrete block walls illuminated by a source outside [11], and imaging through a concrete block wall using the back-projection method [12].

For the TM-polarized incident wave, the method proposed in [9] leads to an approximate result. A rigorous method to characterize the reflection and transmission coefficients for a binary grating periodic medium is proposed in [13]. However, since this method ignores the first-order derivative of the relative permittivity function, it does not give a reliable solution.

In this paper, we propose an exact solution to characterize the reflection and transmission properties of a medium, which is periodic at the center and sandwiched between two uniform layers and illuminated by a TM-polarized plane wave. In contrast to [13], our proposed method does not ignore the first-order derivative of the periodic relative permittivity function. Thus, our method will be a good candidate for the analysis of other types of periodic structures.

This paper is organized as follows: first, the geometry of the

*Corresponding author's email: pdehkhoda@aut.ac.ir

problem is introduced in section 2. Here, we assume that the structure has no variation along the y-axis. The formulation of the solution is given in section 3. The numerical validation of the method is introduced in section 4. Finally, a brief discussion is made in the conclusion section.

2. Problem Geometry

Fig. 1 shows a concrete cinder block used in a typical wall. We assume that the wall extends infinitely along the x-direction and does not have any variations along the y-direction. As in Fig. 1, a three-layer wall is considered; so the problem consists of five regions numbered from 1 to 5. Regions 1 and 5 ($z<0$ and $z>2h_1+2h_2$, respectively) are air. Regions 2 and 4 ($0<z<2h_1$ and $2h_1+h_2<z<2h_1+2h_2$, respectively) are uniform concrete layers with dielectric constants of $\varepsilon_2=\varepsilon_{con}\varepsilon_0$. For region 3 that is periodic with a period of P_x, we set $\varepsilon_2=\varepsilon_{con}\varepsilon_0$ and $\varepsilon_1=\varepsilon_0$ for the dielectric and air regions, respectively. The thickness of the different parts is shown in Fig. 1.

The wall is illuminated by a plane-wave incident in the x-z plane at an angle θ to the z-axis, with a magnetic field polarized along the y-axis (TM-polarized) plane-wave. For this problem the reflected and transmitted field coefficients will be derived.

3- Formulation of the Scattering Problem

According to the Floquet theorem, the periodic layer of the block wall supports an infinite number of Floquet harmonics, having wavenumber $k_{xn}=k_0\sin\theta+2\pi n/P_x$ $(n=0,\pm1,\pm2,\ldots)$ along the x-direction. The $k_0=\omega\sqrt{\mu_0\varepsilon_0}$ is the free-space wavenumber, and μ_0 and ε_0 are vacuum permeability and permittivity constants, respectively. From the phase continuity condition deduced from the boundary equations, the wavenumber along the x-direction will be the same in all regions. Then, the wavenumber along z-direction in each region will be

$$k_{zn,j}=\begin{cases}\sqrt{k_j^2-k_{xn}^2} & , \quad |k_{xn}|<k_j\\ i\sqrt{k_{xn}^2-k_j^2} & , \quad |k_{xn}|>k_j\end{cases} \quad , \quad n=0,\pm1,\pm2,\ldots \tag{1}$$

In (1), k_j is the wavenumber in the j^{th} region (except region 3) defined in section 2, which is equal to $k_0\sqrt{\varepsilon_{con}}$ for regions 2 and 4, and is equal to k_0 for the air at regions 1 and 5.

For the boundary equations, the tangential electromagnetic components in each region should be written. Assuming $e^{-i\omega t}$ time dependence, the tangential electric field will be derived from the tangential magnetic using the second Maxwell's equation as

$$\frac{\partial H_{yj}}{\partial z}=i\omega\varepsilon_0\varepsilon_j E_{xj} \tag{2}$$

where ε_j is the relative dielectric constant in the j^{th} region defined above, which is equal to 1 for regions 1 and 5, ε_{con}

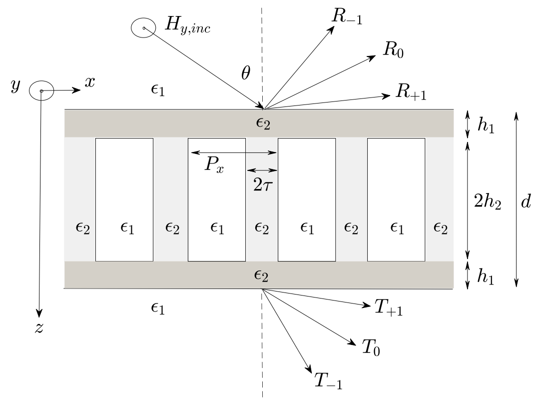

Fig. 1. A concrete block wall illuminated by the TM-polarized incident field. Transmitted and reflected Floquet modes for three modes of $n=-1,0,+1$ are included in the figure to show the non-specular scattering paths.

for regions 2 and 4, and $\varepsilon(x)$ for region 3. In the first region consisting of the incident wave, we have

$$H_{y1}(x,z)=\exp\left(ik_0\left(\sin\theta x+\cos\theta z\right)\right)+\sum_{n\neq0} r_n\exp\left(i\left(k_{xn}x-k_{zn,1}z\right)\right) \tag{3}$$

and in region 5, we have

$$H_{y5}(x,z)=\sum_n t_n\exp\left(i\left(\begin{matrix}k_{xn}x+k_{zn,1}\\ \left(z-(2h_1+2h_2)\right)\end{matrix}\right)\right) \tag{4}$$

where r_n and t_n in (3) and (4) are reflection and transmission coefficients of Floquet harmonics, respectively.

For region 2, the tangential magnetic field component is

$$H_{y2}(x,z)=\sum_n\left[\begin{matrix}I_{2n}^+\exp\left(ik_{zn,2}z\right)+\\ I_{2n}^-\exp\left(-ik_{zn,2}z\right)\end{matrix}\right]\exp\left(ik_{xn}x\right) \tag{5}$$

where I_{2n}^+ and I_{2n}^- are the field amplitudes of the forward and backward traveling waves in the region 2, respectively. Also, for the region 4

$$H_{y4}(x,z)=\sum_n\left[\begin{matrix}I_{4n}^+\exp\left(ik_{zn,2}\left(z-(h_1+2h_2)\right)\right)+\\ I_{4n}^-\exp\left(-ik_{zn,2}\left(z-(h_1+2h_2)\right)\right)\end{matrix}\right]\exp\left(ik_{xn}x\right) \tag{6}$$

where I_{4n}^+ and I_{4n}^- are the field amplitudes of the forward and backward traveling waves in the region 4, respectively.

To derive the tangential electromagnetic field components at the periodic region, we must solve the coupled Maxwell's equations rigorously. For the TM-polarization, these equations are written for the (H_y, E_x, E_z) set of electromagnetic field components in the following form

$$\frac{\partial E_x}{\partial z} - \frac{\partial E_z}{\partial x} = i\omega\mu_0 H_y \tag{7}$$

$$\frac{\partial H_y}{\partial z} = i\omega\varepsilon_0\varepsilon(x)E_x \tag{8}$$

And

$$\frac{\partial H_y}{\partial x} = -i\omega\varepsilon_0\varepsilon(x)E_z \tag{9}$$

The governing differential equations on tangential electromagnetic field components will be derived by eliminating E_z terms. Consider

$$\begin{gathered} E_z = -\frac{1}{i\omega\varepsilon_0}\left(\frac{1}{\varepsilon(x)}\frac{\partial H_y}{\partial x}\right) \Rightarrow \\ \frac{\partial E_z}{\partial x} = \frac{i}{\omega\varepsilon_0}\left[\frac{1}{\varepsilon(x)}\frac{\partial^2 H_y}{\partial x^2} - \frac{d\varepsilon}{dx}\frac{1}{\varepsilon^2(x)}\frac{\partial H_y}{\partial x}\right] \end{gathered} \tag{10}$$

By doing the following steps, the wave equation of the tangential magnetic field component will be derived:

1. Substitute (10) into (7), then multiply both sides of the equation by $\varepsilon^2(x)$.
2. Take the derivative from both sides of (8) with respect to z, then multiply them by $\varepsilon(x)$.
3. Replace the resulting equation in step 1 into the equation derived from step 2.

These steps lead to the wave equation as

$$\begin{gathered} \varepsilon(x)\frac{\partial^2 H_y}{\partial z^2} + k_0^2\varepsilon^2(x)H_y + \\ \left[\varepsilon(x)\frac{\partial^2 H_y}{\partial x^2} - \frac{d\varepsilon}{dx}\frac{\partial H_y}{\partial x}\right] = 0 \end{gathered} \tag{11}$$

The solution of the wave equation in (11) will give the tangential magnetic field, H_y. This equation is valid for all of the Floquet harmonics in the periodic region.

The relative permittivity function, $\varepsilon(x)$, of the periodic region can be written in the form of Fourier series as

$$\varepsilon(x) = \sum_p \varepsilon_p \exp\left(-i\left(\frac{2\pi p}{P_x}x\right)\right) \tag{12}$$

Using this definition, the Fourier series of $\varepsilon^2(x)$ will be

$$\begin{gathered} \varepsilon^2(x) = \left[\sum_p \varepsilon_p \exp\left(-i\left(\frac{2\pi p}{P_x}x\right)\right)\right].\left[\sum_s \varepsilon_s \exp\left(-i\left(\frac{2\pi s}{P_x}x\right)\right)\right] \\ \Rightarrow \varepsilon^2(x) = \sum_p \varepsilon_p \sum_s \varepsilon_s \exp\left(-i\left(\frac{2\pi(p+s)}{P_x}x\right)\right), \end{gathered} \tag{13}$$

by changing the variable $s = f - p$, we will have

$$\begin{gathered} \varepsilon^2(x) = \sum_p \varepsilon_p \sum_f \varepsilon_{(f-p)} \exp\left(-i\left(\frac{2\pi f}{P_x}x\right)\right) \\ \Rightarrow \varepsilon^2(x) = \sum_f \left[\sum_p \varepsilon_{(f-p)}\varepsilon_p\right] \exp\left(-i\left(\frac{2\pi f}{P_x}x\right)\right) \\ \Rightarrow \hat{\varepsilon}_f = \sum_p \varepsilon_{(f-p)}\varepsilon_p . \end{gathered} \tag{14}$$

It means that the Fourier series coefficients of $\varepsilon^2(x)$ are derived by convolving the Fourier series coefficients of $\varepsilon(x)$ with itself. Also, by using some of the Fourier series properties, we have

$$\begin{gathered} \frac{d\varepsilon(x)}{dx} = \sum_p -i\left(\frac{2\pi p}{P_x}\varepsilon_p\right)\exp\left(-i\left(\frac{2\pi p}{P_x}x\right)\right) \Rightarrow \\ \varepsilon_p^x = \frac{2\pi p}{P_x}\varepsilon_p \end{gathered} \tag{15}$$

Now, the tangential magnetic field component in the region 3 can also be expressed with a Fourier expansion in terms of Floquet harmonics as

$$H_{y3}(x,z) = \sum_n U_{yn}(z)\exp\left(ik_{xn}x\right) \tag{16}$$

Replacing (16) into (11) and defining a new variable as $z' = k_0 z$, we have

$$\begin{gathered} \sum_f \varepsilon_{n-f}\frac{\partial^2 U_{yf}}{\partial z'^2} + \sum_f \hat{\varepsilon}_{n-f}U_{yf} - \\ \sum_f \varepsilon_{n-f}\left(\left(\frac{k_{xf}}{k_0}\right)^2 U_{yf}\right) - \sum_f\left(\frac{\varepsilon_{n-f}^x}{k_0}\right)\left(\frac{k_{xf}}{k_0}\right)U_{yf} = 0 \end{gathered} \tag{17}$$

Now, (17) can be written in the matrix form of

$$\overline{\overline{E}}\cdot\frac{\partial^2 \boldsymbol{U}_y}{\partial z'^2} + \overline{\overline{\hat{E}}}\cdot\boldsymbol{U}_y - \overline{\overline{E}}\cdot\overline{\overline{K}}_x^2\cdot\boldsymbol{U}_y - \overline{\overline{E}}_x\cdot\overline{\overline{K}}_x\cdot\boldsymbol{U}_y = 0 \tag{18}$$

where the constituent elements of the matrices in (18) can be determined by one-to-one comparison of (17) with (18). The final form of the equation in (18) is as follows

$$\frac{\partial^2 \boldsymbol{U}_y}{\partial z'^2} + \overline{\overline{A}} \cdot \boldsymbol{U}_y = 0 \tag{19}$$

where,

$$\overline{\overline{A}} = \left[\overline{\overline{E}}^{-1} \cdot \overline{\overline{\widehat{E}}} - \left(\overline{\overline{K}}_x^{2} + \overline{\overline{E}}^{-1} \cdot \overline{\overline{E}}_x \cdot \overline{\overline{K}}_x \right) \right] \tag{20}$$

The matrix form of the second-order differential equation in (19) can be solved if $\overline{\overline{A}}$ in (20) is diagonalizable. The solution of (19) leads to tangential magnetic Floquet harmonics in the form of

$$U_{yn}(z) = \sum_m w_{n,m} \left\{ \begin{array}{l} c_m^+ \exp\left(ik_0 q_m \left(z-(h_1+h_2)\right)\right) + \\ c_m^- \exp\left(-ik_0 q_m \left(z-(h_1+h_2)\right)\right) \end{array} \right\} \tag{21}$$

In (21), $w_{n,m}$ and q_m are elements of $\overline{\overline{W}}$ and $\overline{\overline{Q}}$ matrices, respectively. Please note that, $\overline{\overline{W}}$ is the eigenmatrix of $\overline{\overline{A}}$. In addition, q_m are the positive square root of the eigenvalues of $\overline{\overline{A}}$, which are also diagonal elements of the diagonal matrix of $\overline{\overline{Q}}$. The c_m^+ and c_m^- in (21) are the unknown coefficients that will be derived from the boundary condition equations.

The boundary equations are derived at $z=0$, $z=h_1$, $z=h_1+2h_2$ and $z=2h_1+2h_2$. For a source-free problem, these equations are written based on the continuity of tangential electromagnetic field components, where for the TM-polarization case are H_y and E_x. The resulting equations are as follows

$$\delta_{n0} + r_n = I_{2n}^+ + I_{2n}^- \tag{22}$$

$$Z_{1,n}\left(\delta_{n0} + r_n\right) = Z_{2,n}\left(I_{2n}^+ + I_{2n}^-\right) \tag{23}$$

$$\begin{array}{l} I_{2n}^+ \exp\left(ik_{zn,2}h_1\right) + I_{2n}^- \exp\left(-ik_{zn,2}h_1\right) = \\ \sum_m w_{n,m}\left\{c_m^+ \exp\left(-ik_0 q_m h_2\right) + c_m^- \exp\left(ik_0 q_m h_2\right)\right\} \end{array} \tag{24}$$

$$\begin{array}{l} Z_{2,n}\left[I_{2n}^+ \exp\left(ik_{zn,2}h_1\right) - I_{2n}^- \exp\left(-ik_{zn,2}h_1\right)\right] = \\ \sum_m v_{n,m}\left\{c_m^+ \exp\left(-ik_0 q_m h_2\right) - c_m^- \exp\left(ik_0 q_m h_2\right)\right\} \end{array} \tag{25}$$

$$\sum_m w_{n,m}\left\{c_m^+ \exp\left(ik_0 q_m h_2\right) + c_m^- \exp\left(-ik_0 q_m h_2\right)\right\} = I_{4n}^+ + I_{4n}^- \tag{26}$$

$$\begin{array}{l} \sum_m v_{n,m}\left\{c_m^+ \exp\left(ik_0 q_m h_2\right) - c_m^- \exp\left(-ik_0 q_m h_2\right)\right\} = \\ Z_{4,n}\left[I_{4n}^+ - I_{4n}^-\right] \end{array} \tag{27}$$

$$\left[I_{4n}^+ \exp\left(ik_{zn,4}h_1\right) + I_{4n}^- \exp\left(-ik_{zn,4}h_1\right)\right] = t_n \tag{28}$$

And

$$Z_{4,n}\left[I_{4n}^+ \exp\left(ik_{zn,2}h_1\right) - I_{4n}^- \exp\left(-ik_{zn,4}h_1\right)\right] = Z_{5,n} t_n \tag{29}$$

where $\eta_0 = \sqrt{\mu_0/\varepsilon_0}$ is the impedance of free space. Also

$$Z_{1,n} = Z_{5,n} = \eta_0 \frac{k_{zn,1}}{k_0} \tag{30}$$

And

$$Z_{2,n} = Z_{4,n} = \eta_0 \frac{k_{zn,2}}{k_0 \varepsilon_{con}} \tag{31}$$

The terms $v_{n,m}$ are elements of the matrix $\overline{\overline{V}}$ that can be derived as

$$\overline{\overline{V}} = \eta_0 \cdot \overline{\overline{E}}^{-1} \cdot \overline{\overline{W}} \cdot \overline{\overline{Q}} \tag{32}$$

The matrix form of boundary equations written in (22) to (29) are in the form of

$$\delta_{n0} + \boldsymbol{R} = \boldsymbol{I}_2^+ + \boldsymbol{I}_2^- \tag{33}$$

$$\left(\frac{\cos\theta}{\eta_0}\right) \cdot \delta_{n0} - \overline{\overline{Z}}_1 \cdot \boldsymbol{R} = \overline{\overline{Z}}_2 \cdot \left(\boldsymbol{I}_2^+ - \boldsymbol{I}_2^-\right) \tag{34}$$

$$\overline{\overline{E}}_{k2} \cdot \boldsymbol{I}_2^+ + \overline{\overline{E}}_{k2}^{-1} \cdot \boldsymbol{I}_2^- = \overline{\overline{W}} \cdot \left(\overline{\overline{E}}_{k3}^{-1} \cdot \boldsymbol{c}^+ + \overline{\overline{E}}_{k3} \cdot \boldsymbol{c}^-\right) \tag{35}$$

$$\overline{\overline{Z}}_2 \cdot \left(\overline{\overline{E}}_{k2} \cdot \boldsymbol{I}_2^+ - \overline{\overline{E}}_{k2}^{-1} \cdot \boldsymbol{I}_2^-\right) = \overline{\overline{V}} \cdot \left(\overline{\overline{E}}_{k3}^{-1} \cdot \boldsymbol{c}^+ - \overline{\overline{E}}_{k3} \cdot \boldsymbol{c}^-\right) \tag{36}$$

$$\overline{\overline{W}} \cdot \left(\overline{\overline{E}}_{k3} \cdot \boldsymbol{c}^+ + \overline{\overline{E}}_{k3}^{-1} \cdot \boldsymbol{c}^-\right) = \boldsymbol{I}_4^+ + \boldsymbol{I}_4^- \tag{37}$$

$$\overline{\overline{V}} \cdot \left(\overline{\overline{E}}_{k3} \cdot \boldsymbol{c}^+ - \overline{\overline{E}}_{k3}^{-1} \cdot \boldsymbol{c}^-\right) = \overline{\overline{Z}}_2 \cdot \left(\boldsymbol{I}_4^+ - \boldsymbol{I}_4^-\right) \tag{38}$$

$$\overline{\overline{E}}_{k2} \cdot \boldsymbol{I}_4^+ + \overline{\overline{E}}_{k2}^{-1} \cdot \boldsymbol{I}_4^- = \boldsymbol{T} \tag{39}$$

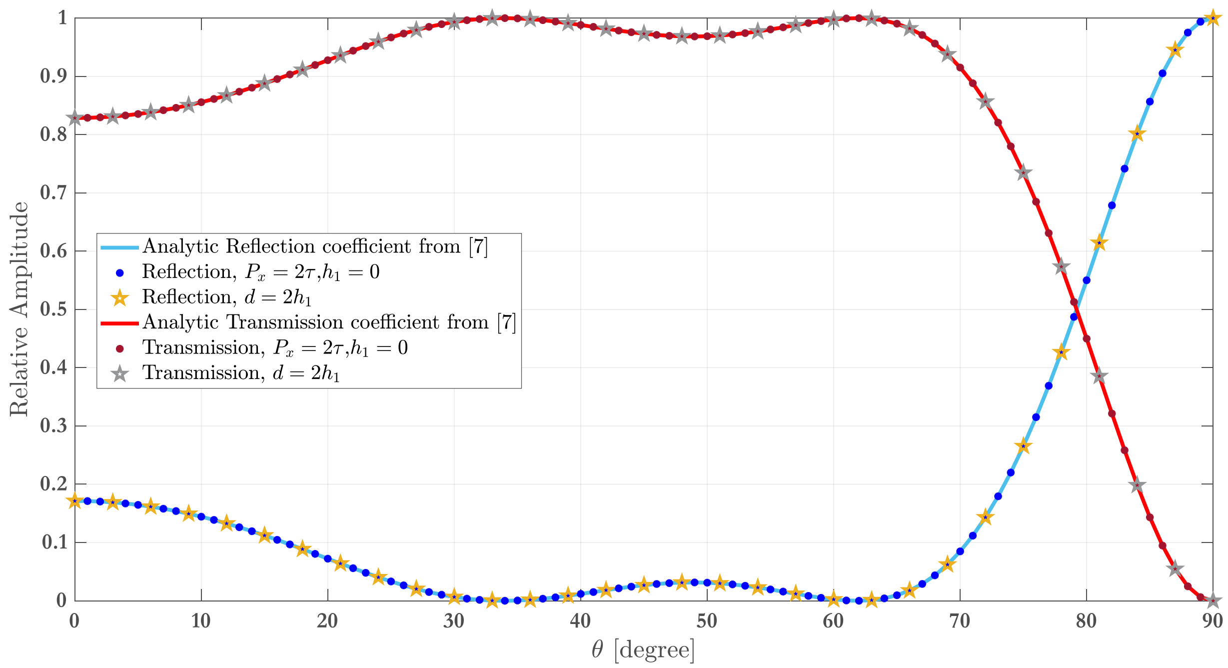

Fig. 2. Comparison of the reflection and transmission coefficients between the proposed method and the analytical method in [14] for the dielectric slab case of the problem of Fig. 1 with 20 cm thickness and $\varepsilon_2 = 3.5$ ($h_1 = 0,\ P_x = 2\tau$ or $d = 2h_1$)

And

$$\overline{\overline{Z}}_2 \cdot \left(\overline{\overline{E}}_{k2} \cdot \boldsymbol{I}_4^+ - \overline{\overline{E}}_{k2}^{-1} \cdot \boldsymbol{I}_4^- \right) = \overline{\overline{Z}}_1 \cdot \boldsymbol{T} \tag{40}$$

In (33) to (40), $\overline{\overline{Z}}_1$, $\overline{\overline{Z}}_2$, $\overline{\overline{E}}_{k2}$ and $\overline{\overline{E}}_{k3}$ are diagonal matrices which their diagonal elements are $k_{zn,1}/k_0\eta_0$, $k_{zn,2}/k_0\eta_0\varepsilon_{con}$, $\exp\left(ik_{zn,2}h_1\right)$ and $\exp\left(ik_{zn,2}h_2\right)$, respectively. Also, the unknown vectors $\boldsymbol{R}$, $\boldsymbol{T}$, $\boldsymbol{I}_2^+$, $\boldsymbol{I}_2^-$, $\boldsymbol{I}_4^+$, $\boldsymbol{I}_4^-$, $\boldsymbol{c}^+$ and $\boldsymbol{c}^-$ are vectors whose elements are r_n, t_n, I_{2n}^+, I_{2n}^-, I_{4n}^+, I_{4n}^-, c_m^+ and c_m^-, respectively.

To compute the unknowns $\boldsymbol{R}$ and $\boldsymbol{T}$, auxiliary matrices can first be defined. Let

$$\overline{\overline{R}}_B = \left(\overline{\overline{Z}}_2 + \overline{\overline{Z}}_1 \right)^{-1} \cdot \left(\overline{\overline{Z}}_1 - \overline{\overline{Z}}_2 \right) \tag{41}$$

$$\overline{\overline{R}}_T = \left(\overline{\overline{Z}}_2 - \overline{\overline{Z}}_1 \right)^{-1} \cdot \left(\overline{\overline{Z}}_1 + \overline{\overline{Z}}_2 \right) = -\overline{\overline{R}}_B^{-1} \tag{42}$$

The matrices in (41) and (42), are diagonal matrices for regions 4 and 2 uniform dielectric layers, respectively, which are interpreted as the field reflection coefficients looking up into the air from their respective dielectric layers.

Also for convenience, we define

$$\overline{\overline{M}}_1 = \overline{\overline{W}} + \overline{\overline{Z}}_2^{-1} \cdot \overline{\overline{V}} \tag{43}$$

$$\overline{\overline{M}}_2 = \overline{\overline{W}} - \overline{\overline{Z}}_2^{-1} \cdot \overline{\overline{V}} \tag{44}$$

$$\overline{\overline{R}}_{BF} = -\overline{\overline{E}}_{k3} \cdot \left(\overline{\overline{M}}_1 + \overline{\overline{E}}_{k2} \cdot \overline{\overline{R}}_B \cdot \overline{\overline{E}}_{k2} \cdot \overline{\overline{M}}_2 \right)^{-1} \cdot \left(\overline{\overline{M}}_2 + \overline{\overline{E}}_{k2} \cdot \overline{\overline{R}}_B \cdot \overline{\overline{E}}_{k2} \cdot \overline{\overline{M}}_1 \right) \cdot \overline{\overline{E}}_{k3} \tag{45}$$

$$\overline{\overline{C}}_1 = \left(\overline{\overline{M}}_1 \cdot \overline{\overline{E}}_{k3}^{-1} + \overline{\overline{M}}_2 \cdot \overline{\overline{E}}_{k3} \cdot \overline{\overline{R}}_{BF} \right)^{-1} \tag{46}$$

And

$$\overline{\overline{C}}_2 = \left(\overline{\overline{M}}_2 \cdot \overline{\overline{E}}_{k3}^{-1} + \overline{\overline{M}}_1 \cdot \overline{\overline{E}}_{k3} \cdot \overline{\overline{R}}_{BF} \right)^{-1} \tag{47}$$

Using the above matrices in (41) to (47), the required unknowns $\boldsymbol{R}$ and $\boldsymbol{T}$ will be derived from (33) to (39). The resulting solution is as follows

$$\boldsymbol{R} = \left(\overline{\overline{I}} + \overline{\overline{R}}_T \right) \cdot \left[-\overline{\overline{R}}_T + \overline{\overline{E}}_{k2} \cdot \overline{\overline{C}}_2^{-1} \cdot \overline{\overline{C}}_1 \cdot \overline{\overline{E}}_{k2} \right]^{-1} \cdot \left(\overline{\overline{I}} - \overline{\overline{R}}_T \right) \cdot \delta_{n0} - \overline{\overline{R}}_T \cdot \delta_{n0} \tag{48}$$

And

$$\boldsymbol{T} = \left(\overline{\overline{I}} - \overline{\overline{R}}_B \right) \cdot \overline{\overline{E}}_{k2} \cdot \left[\overline{\overline{M}}_1 \cdot \overline{\overline{E}}_{k3} + \overline{\overline{M}}_2 \cdot \overline{\overline{E}}_{k3} \cdot \overline{\overline{R}}_{BF} \right] \cdot \left(\overline{\overline{C}}_1 \cdot \overline{\overline{E}}_{k2} \right) \cdot \left[-\overline{\overline{R}}_T + \overline{\overline{E}}_{k2} \cdot \overline{\overline{C}}_2^{-1} \cdot \overline{\overline{C}}_1 \cdot \overline{\overline{E}}_{k2} \right]^{-1} \cdot \left(\overline{\overline{I}} - \overline{\overline{R}}_T \right) \cdot \delta_{n0} \tag{49}$$

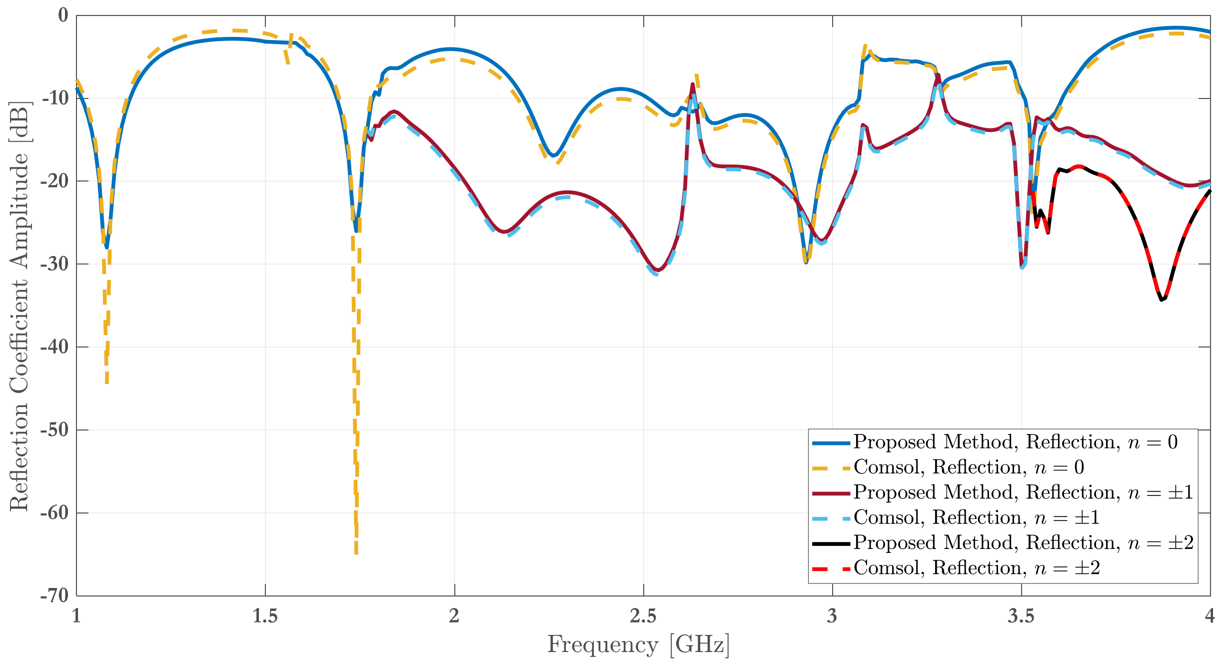

Fig. 3. Comparison of the reflection coefficients of harmonic Floquet modes between the proposed method and Comsol for the problem of Fig. 1 with 20 cm thickness and $\varepsilon_2 = 3.5$ ($h_1 = 2\tau = 4$ cm **and** $P_x = d = 20$ cm)

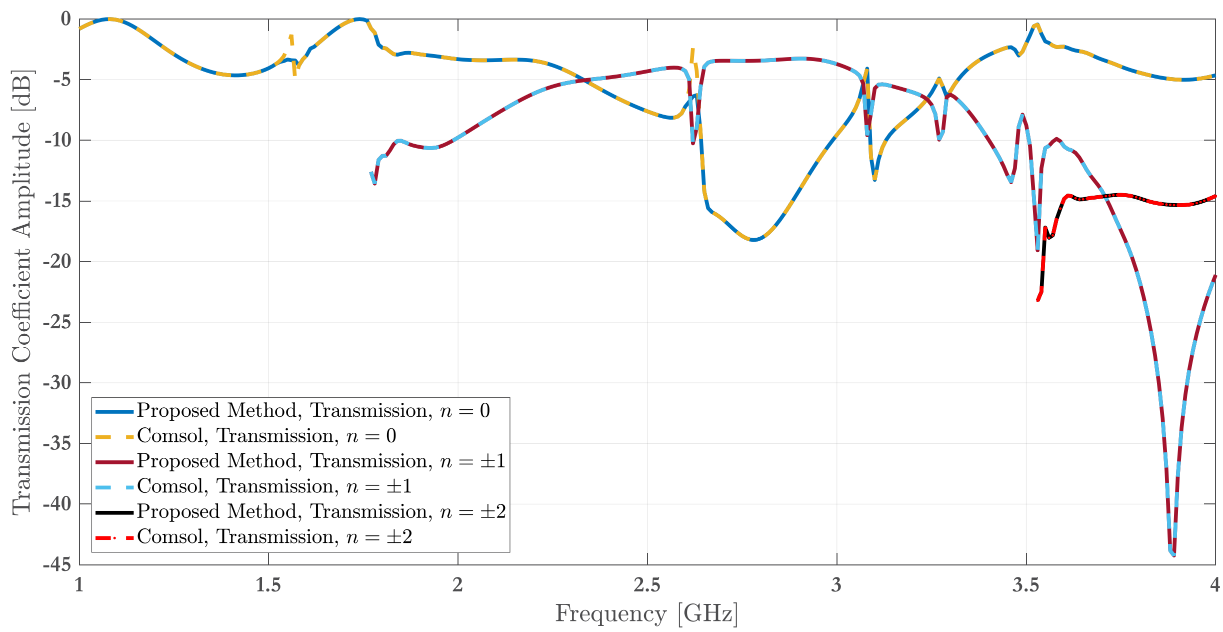

Fig. 4. Comparison of the transmission coefficients of harmonic Floquet modes between the proposed method and Comsol for the problem of Fig. 1 with 20 cm thickness and $\varepsilon_2 = 3.5$ ($h_1 = 2\tau = 4$ cm **and** $P_x = d = 20$ cm)

From the vectors $\boldsymbol{R}$ and $\boldsymbol{T}$, we obtain the reflection and transmission coefficients for the Floquet harmonics.

4- Numerical Validation

Two types of comparisons are made to validate the proposed formulation. In the first case, we assume that the wall is a uniform homogeneous layer, so we can compare the obtained results with the ones in the literature. Wall parameters in Fig. 1 are set to $P_x = 2\tau = 20$ cm, $\varepsilon_1 = 1$, $\varepsilon_2 = 3.5$, $d = 20$ cm . In this case, can be either zero or $d/2$. Then, calculated reflection and transmission coefficients are compared with the ones obtained by an analytical solution in [14]. The wall is illuminated by an incident plane wave at an arbitrary frequency of 3 GHz. The results are depicted in Fig. 2 as a function of incident angle, θ , varying between 0 and 90. As observed an excellent agreement exists between the results.

As the second case, we consider a periodic concrete block wall with $P_x = 20$ cm , $2\tau = h_1 = 4$ cm , $d = 20$ cm , $\varepsilon_2 = 3.5$ and $\varepsilon_1 = 1$. The structure is illuminated by a normal incident plane wave, swept from 1 GHz to 4 GHz. We consider a total number of 51 Floquet modes in our computation. Fig. 3 and 4 show reflection and transmission coefficients of the first five propagating Floquet modes. Calculated results are compared with the numerical results derived from Comsol© software. As observed, the results are in good agreement with each other.

5-Conclusion

In this paper, a rigorous method was introduced to study the electromagnetic behavior of a periodic wall under the illumination of an oblique TM-polarized plane wave. Floquet theory together with Fourier series representation of the relative dielectric function of the periodic layer are the principal tools used to aid the solution of the boundary value problem and find the scattering coefficients. Numerical validation of the problem was also presented. The ability to calculate Fourier series coefficients by taking FFT of the relative permittivity function enables the introduced method to treat any type of periodic inhomogeneities.

It is worth mentioning that the assumption made during the solution process which accounts for no variation of the wall along the y-direction is not quite applicable in reality for some cases. The solution of a wall which varies along both x- and y-directions will be presented in the future works.

Nomenclature

t time
E_x electric field component in the x-direction, V/m
E_z electric field component in the z-direction, V/m
H_y magnetic field component in the y-direction, A/m
ε_0 permittivity of free-space, F/m
$\varepsilon(x)$ relative dielectric function of the inhomogeneous periodic layer
η_0 characteristic impedance of free-space, Ω
μ_0 permeability of free-space, H/m
ω angular frequency, rad/s

References

[1] Burkholder R.J., Marhefka R.J., Volakis J.L. (2008). Radar imaging through cinder block walls and other periodic structures. *2008 IEEE Antennas and Propagation Society International Symposium*, IEEE, 1-4.

[2] Burkholder R.J., Volakis J.L. (2009). Time-reversal radar imaging through periodic structures. *2009 IEEE Antennas and Propagation Society International Symposium*, IEEE, 1-4.

[3] Holloway C.L., Perini P.L., DeLyser R.R., Allen K.C. (1997). Analysis of composite walls and their effects on short-path propagation modeling. *IEEE Transactions on Vehicular Technology*, 46(3): 730-738.

[4] Iskander M.F., Yun Z. (2002). Propagation prediction models for wireless communication systems. *IEEE Transactions on microwave theory and techniques*, 50(3): 662-673.

[5] Sarkar T.K., Ji Z., Kim K., Medouri A., Salazar-Palma M. (2003). A survey of various propagation models for mobile communication. *IEEE Antennas and propagation Magazine*, 45(3): 51-82.

[6] Lim S.Y., Yun Z., Iskander M.F. (2018). Radio Propagation Modeling: A Unified View of the Ray-Tracing Image Method Across Emerging Indoor and Outdoor Environments. *The World of Applied Electromagnetics*, Springer, 301-328.

[7] Teh C., Chung B., Lim E. (2019). Multilayer Wall Correction Factors for Indoor Ray-Tracing Radio Propagation Modeling. *IEEE Transactions on Antennas and Propagation*, 68(1): 604-608.

[8] Honcharenko W., Bertoni H.L. (1994). Transmission and reflection characteristics at concrete block walls in the UHF bands proposed for future PCS. *IEEE Transactions on Antennas and Propagation*, 42(2): 232-239.

[9] Peng S., Tamir T., Bertoni H.L. (1975). Theory of periodic dielectric waveguides. *IEEE Transactions on Microwave Theory and Techniques*, 23(1): 123-133.

[10] Bertoni H.L., Cheo L.-H.S., Tamir T. (1989). Frequency-selective reflection and transmission by a periodic dielectric layer. *IEEE Transactions on Antennas and Propagation*, 37(1): 78-83.

[11] Khorashadi-Zadeh V., Omrani A., Dehmollaian M. (2018). Scattered Fields of a 2-D Rectangular Room Composed of Cinder Block Walls Using Floquet–Fourier Series Expansion. *IEEE Transactions on Antennas and Propagation*, 67(1): 390-399.

[12] Khorashadi-Zadeh V., Dehmollaian M. (2018). Through a cinder block wall refocusing using SAR back-projection method. *IEEE Transactions on Antennas and Propagation*, 67(2): 1212-1222.

[13] Moharam M., Grann E.B., Pommet D.A., Gaylord T. (1995). Formulation for stable and efficient implementation of the rigorous coupled-wave analysis of binary gratings, *JOSA A*, 12(5): 1068-1076.

[14] Kong J.A. (1986). *Electromagnetic Wave Theory*. Wiley.

HOW TO CITE THIS ARTICLE

A. Ahmadi, P. Dehkhoda, A. Tavakoli, M. Dehmollaian, Transmission and Reflection Characteristics of a Concrete Block Wall Illuminated by a TM-polarized Obliquely incident wave, AUT J. Elec. Eng., 52(2) (2020) 179-186.

DOI: 10.22060/eej.2020.18432.5353